C. R. Biologies 340 (2017) 25–36

Contents lists available at ScienceDirect

Comptes Rendus Biologies

www.sciencedirect.com

Animal biology and pathology/Biologie et pathologie animales

High carbohydrate diet induces nonalcoholic steato-hepatitis (NASH) in a desert gerbil

Induction d'une stéatose hépatique non alcoolique par une alimentation hyperglucidique chez une gerbille désertique

Nesrine Semiane [a,*], Fabienne Foufelle [b,c,d], Pascal Ferré [b,c,d], Isabelle Hainault [b,c], Souad Ameddah [e], Aicha Mallek [a], Ali Khalkhal [a], Yasmina Dahmani [a]

[a] *LBPO/Nutrition-métabolisme, FSB/USTHB, BP 32, El Alia, 16111 Alger, Algeria*
[b] *INSERM, UMR-S 872, centre de recherches des Cordeliers, 75006 Paris, France*
[c] *Université Paris-6–Pierre-et-Marie-Curie, UMR S 872, 75006 Paris, France*
[d] *Université Paris-Descartes, UMR S 872, 75006 Paris, France*
[e] *Laboratoire de biologie et environnement, université Mentouri, route de Ain El Bey, 25000 Constantine, Algeria*

ARTICLE INFO

Article history:
Received 11 July 2016
Accepted after revision 7 September 2016
Available online 30 September 2016

Keywords:
Gerbillus gerbillus
Insulin resistance
Lipogenesis
E.R. stress
Oxidative stress

ABSTRACT

A high intake of sugars has been linked to diet-induced health problems. The aim of this study was to assess whether the long-term consumption of a high-carbohydrate diet (HCD) would cause the hepatic histopathological and metabolic abnormalities that characterize nonalcoholic steatohepatitis (NASH) in a desert gerbil, *Gerbillus gerbillus*. Compared to natural diet, HCD leads to several metabolic disorders including adiposity, dyslipidemia, insulin resistance, ectopic fat deposition in the liver, which were associated with higher levels of transcripts of genes involved with fat synthesis, endoplasmic reticulum (ER) stress, and fibrosis. In the same way, the experimented animals showed enhanced oxidative stress. Taken together, these results demonstrate that HCD consumption in gerbils induces metabolic disorders and damaged liver, which are key contributors to NASH development. These results suggest that this rodent represents a valuable natural model for human diet-induced metabolic disorders and nonalcoholic fatty liver disease (NAFLD).

Mots clés :
Gerbillus gerbillus
Insulino-résistance
Lipogenèse
Stress R.E.
Stress oxydatif

RÉSUMÉ

Les effets d'un régime riche en hydrates de carbone (RHC) sur l'induction de dysfonctionnements métaboliques et d'altérations histopathologiques au niveau du foie caractérisant la stéatose hépatique non alcoolique (NASH) ont été étudiés chez la gerbille *Gerbillus gerbillus*. Comparativement au régime naturel, l'alimentation hyperglucidique induit des perturbations métaboliques marquées par une adiposité, une dyslipidémie, une insulinorésistance et un dépôt ectopique de graisses dans le foie, associé à l'augmentation des ARNm de gènes impliqués dans la synthèse des lipides, le stress du réticulum

* Corresponding author.
E-mail address: semianenesrine@yahoo.fr (N. Semiane).

http://dx.doi.org/10.1016/j.crvi.2016.09.002
1631-0691/

endoplasmique et la fibrose. Parallèlement, les animaux expérimentaux développent un état de stress oxydatif. Le RHC induit chez *G. gerbillus* des troubles métaboliques et des lésions hépatiques caractéristiques de la NASH. Nos résultats suggèrent que ce rongeur représente un modèle naturel de choix pour l'étude des dysfonctionnements métaboliques et hépatiques induits par une consommation excessive de glucides chez l'humain.

1. Introduction

Nonalcoholic fatty liver disease (NAFLD) is the main cause of hepatic dysfunction in developed countries and is closely related to components of metabolic syndrome such as obesity, dyslipidemia and type-2 diabetes [1]. Excessive accumulation of triglyceride (TG) in hepatocytes is the hallmark of NAFLD. The spectrum of NAFLD ranges from hepatic steatosis or fatty liver to nonalcoholic steatohepatitis (NASH), liver fibrosis, liver cirrhosis, and eventually hepatocellular carcinoma (HCC) [2]. The precise mechanisms of NAFLD remain poorly understood. The "multiple-hit hypothesis" is currently the most recognized theory to explain disease development and progression, the dysregulation in lipid metabolism being involved in the first hit [3]. It was estimated that 30 % of the TG content in NAFLD livers came from *de novo* lipogenesis, underlying the importance of this pathway in the etiology of NAFLD [4,5]. De novo lipogenesis (DNL) can be triggered by multiple mechanisms, including increased expression of lipogenic enzymes by several specific transcription factors; this is particularly true for members of the SREBP family. One of them, SREBP-1c, controls hepatic DNL primarily by regulation of expression of genes involved in DNL, lipid homeostasis and glucose metabolism [5,6]. Accordingly, hepatic expression of SREBP-1c and its target genes are increased in human fatty liver, compared to healthy individuals [7,8], although DNL is an important determinant of steatosis [9]. The second of the two hits could be due to (1) oxidative stress, (2) proinflammatory cytokines, (3) mitochondrial dysfunction, or/and (4) endoplasmic reticulum stress. Recently, accumulating data have implicated the disruption of endoplasmic reticulum (ER) homeostasis, or ER stress, in both the development of steatosis and progression to NASH [10,11]. ER stress may lead to the activation of various intracellular stress pathways that can initiate or exacerbate insulin resistance (IR) and inflammation and, in some cases, culminate in hepatocyte cell death and liver damage, all of which are important in the pathogenesis of NAFLD. In spite of growing knowledge, several aspects of NAFLD pathogenesis are still unknown.

Considering the difficulty in developing human studies to evaluate the influence of nutrition in the development of NAFLD and associated metabolic abnormalities, animal models constitute a reliable alternative way. Different animal models of NAFLD/NASH have been developed, but few of them replicate the entire human phenotype [12,13]. These models may be classified into three basic categories: those caused by either spontaneous or induced genetic mutation; those produced by either dietary or pharmacological manipulation; and those involving genetic mutation and dietary or chemical challenges. The dietary manipulations used in these last two types of models usually do not resemble the human dietary pattern.

The aim of this study was to determine the long-term impact of high-carbohydrate diet on liver morphology and function in a desert rodent (*Gerbillus gerbillus*). We therefore evaluated the markers involved in metabolic functions, i.e. lipogenesis, fibrosis, ER stress, histopathological changes, and oxidative stress. In the present study, we developed a model of obesity and obesity-related NAFLD in a desert rodent (*G. gerbillus*) using a simple carbohydrate-rich diet.

2. Materials and methods

2.1. Animals and diets

G. gerbillus individuals were collected from the semi-desert Algerian region of Beni-Abbes (30°7' latitude north and 2°10' longitude west). The authorization to capture the animals in desert region was given by the Ministry of Higher Education (Algeria). *G. gerbillus* specimens were maintained under controlled temperature (22 ± 1 °C), humidity (50%) with a fixed 12-h light/dark cycle. After two weeks of acclimatation, the adult gerbils of both sexes were randomly divided into two groups. The control group (n = 6) received a natural diet composed of halophile fresh plants, seeds, dry plants... whereas the experimental group (n = 6) received an HC diet (25 % of barley and 75 % of dried dates) corresponding to a daily caloric intake of 22.5 calories/animal. Details of the composition of the high-carbohydrate diet (HCD) are presented in Table 1. After six months of diet

Table 1
Diet compositions according to Nicole Tonelli and François Gallouin, Fruit and seeds comestibles worldwide, 7th edition. MedPharm Scientific Publishers/Taylor & Francis, 2008.

Nutritional composition	Barley (g/100 g)	Dried dates (g/100 g)
Carbohydrates	**63.30**	**65**
Starch	61.59	–
Simple sugars	1.71	
Glucose	–	25
Fructose	–	25
Saccharose	–	14
Sorbitol	–	1
Protein	11.2	2
Lipids	2.1	0.5
Water	12.2	20
Fibers	9.8	9
Vitamins	0.015	0.012
Minerals & Trace Elements	0.956	0.862
Calories	314 kcal	275 kcal

administration, the animals were killed by decapitation. The livers and fat pads (mesenteric. genital and perirenal) were totally removed, rinsed with cold 0.9 % NaCl, weighed, and cut. One part of the liver was fixed in 10% neutral buffered formalin for histopathological investigations. The other part was first frozen in liquid nitrogen and then stored at–80 °C for later use in biochemical studies.

2.2. Biochemical analyses

Blood samples were collected after 24 weeks of feeding by puncture from the retro-orbital venous plexus into heparinized or EDTA-containing tubes. The plasma was immediately separated by centrifugation at 3000 *g* for 10 min and rapidly stored at–20 °C until analysis. Plasma glucose, total cholesterol, triacylglycerol (TG), HDL cholesterol and reliable markers of hepatic function (aspartate aminotransferase, AST; alanine aminotransferase, ALT) were measured by using the corresponding kits for analysis (Spinreact, Spain). Plasma LDL cholesterol concentration was calculated by using the equation of Friedewald. Plasma insulin was measured by radioimmunoassay (INSULIN-CT kit, Cisbio assay, France). Homeostasis model assessment of insulin resistance (HOMA-IR) was calculated according to the following formula: HOMA-IR = fasting insulin (μU/mL) × fasting glucose (mmol/L)/22.5.

2.3. Histopathology

A portion of liver (100 mg) was fixed with 10% formalin for 24 h, dehydrated in graded ethanol, and embedded in paraffin. The samples were cut into 5-μm-thick sections and stained with Masson's trichrome for evaluation by light microscopy for fibrotic deposition.

2.4. Hepatic lipid analyses

Liver total lipids were extracted by the method of Folch et al. [14]. The concentrations of triglycerides and cholesterol in the hepatic lipid extracts were measured using the same enzymatic kits as those used for plasma analysis.

3. Estimation of hepatic oxidative stress

3.1. Liver homogenate preparation

Liver samples from each gerbil were homogenized in Tris/EDTA buffer (50 mM Tris. 0.1 mM EDTA. pH 7.6) to obtain a 10% (w/v) liver homogenate. An aliquot of tissue homogenate was centrifuged at 1,000 rpm for 5 min at 4 °C for the estimation of MDA (malondialdehyde). The remaining volume of homogenate was centrifuged at 9,600 rpm for 20 min at 4 °C. The supernatant was collected and used for the estimation of GSH (reduced glutathione), and for measuring the activity of SOD (superoxide dismutase), CAT (catalase), and GST (glutathione-*S*-transferase).

3.2. Markers of lipid peroxidation

Lipid peroxidation was assessed indirectly by the measurement of secondary products malondialdehyde (MDA) using a thiobarbituric acid (TBA) method according to the protocol. MDA formed a colored complex in the presence of thiobarbituric acid, which was detected by spectrophotometrical measurement of the absorbance at 535 nm [15].

3.3. Evaluation of antioxidant enzyme activity

3.3.1. Activity of SOD

Superoxide dismutase was estimated using the method described in [16]. Superoxide anions are generated during the oxidation of pyrogallol under test conditions and SOD enzyme inhibits the oxidation of pyrogallol. The enzyme activity is measured by monitoring the rate of decrease in optical density at 420 nm. One unit of enzyme was defined as the amount of enzyme required to produce 50% inhibition of pyrogallol autoxidation under the assay conditions and expressed as U/mg protein.

3.3.2. Activity of catalase

Catalase activity was assayed by the method of Aebi [17]. The rate of H_2O_2 decomposition was followed by monitoring absorption at 240 nm. The enzyme activity was expressed as millimoles of H_2O_2 consumed per minute per milligram of protein.

3.3.3. Activity of GST

GST activity was measured using the method of Habig et al. [18]. Briefly, 1 mM CDNB was added to a buffer solution containing 1 mM GSH and an aliquot of the sample to be tested. Upon addition of CDNB, the change in absorbance at 340 nm was measured as a function of time. The extinction coefficient for this reaction is 9.6 $mM^{-1} \cdot cm^{-1}$.

3.3.4. Concentration of GSH

GSH level was estimated using a colorimetric technique as mentioned by Ellman [19], based on the development of a yellow color when 5,5-dithio-bis-(2-nitrobenzoic acid) (DTNB) is added to compounds containing sulfhydryl groups. Absorbance was recorded at 412 nm. The total GSH content was expressed as nanomoles of GSH per milligram of protein.

3.4. Protein estimation

The protein content was determined using Bradford's method [20], bovine serum albumin being taken as the standard.

3.5. RNA extraction and RT-qPCR

Total RNA was isolated according to [21]. Real-time quantitative RT-PCR analyses were performed with 50 ng of cDNA/3 mM MgCl2/250 nM sense and antisense primers (Proligo, Boulder, CO, USA) in a final reaction volume of 25 μl by using the qPCR TM Core Kit (Eurogentec, Brussels) and the MyiQ real-time PCR detection system (Bio-Rad). Specific primers were designed with Primer Express software (Table 2). The relative quantitation of each gene was calculated after normalization to 18S ribosomal RNA by using the comparative CT method.

Table 2
Sequences of the primers used for quantitative real-time PCR.

Genes	primer sequenses
FAS	
Sense	5′-tgc tcc cag ctg cag gc -3′
AntiSense	5′-gcc cgg tag ctc tgg gtg ta-3′
SREBP1c	
Sense	5′-gga gcc atg gat tgc aca tt-3′
AntiSense	5′-ggc ccg gga agt cac tgt-3′
ACC	
Sense	5′-tgg gca cag acc gtg gta g-3′
AntiSense	5′-ggt ctt aaa tgc aga gtc tgg gaa-3′
SREBP2	
Sense	5′-ccc ttg act tcc ttg ctg ca-3′
AntiSense	5′-gcg tga gtg tgg gcg aat c-3′
HMG CoA synthase	
Sense	5′-gcc gtg aac tgg gtc gaa-3′
AntiSense	5′-gca tat ata gca atg tct cct gca a-3′
HMG CoA reductase	
Sense	5′-gat tct ggc agt cag tgg gaa-3′
AntiSense	5′-gtt gta gcc gcc tat gct cc-3′
aSma	
Sense	5′-ttg gaa aag atc tgg cac cac-3′
AntiSense	5′-gca gta gtc acg aag gaa tag-3′
Col1A1	
Sense	5′-ccc cgg gac tcc tgg act t-3′
AntiSense	5′-gctccgacacgcccctctctc-3′
TGF-β	
Sense	5′-gcctgagtggctgtcttttgac-3′
AntiSense	5′-catggatggtgcccaggt-3′
GRP78	
Sense	5′-gaa agg atg gtt aat gat gct gag-3′
AntiSense	5′-gtc ttc aat gtc cgc atc ctg-3′
ORP150	
Sense	5′-tgt cct ctt ggc aga cct gtt g-3′
AntiSense	5′-ttt tcc tcc gag att cct tgt tc-3′
18S	
Sense	5′-ggg agc ctg aga aac ggc-3′
AntiSense	5′-ggg tcg gga gtg ggt aat tt-3′

3.6. Preparation of nuclear extracts

Nuclear extracts were prepared as described in [22]. Livers were removed and quickly rinsed in an ice-cold phosphate-buffered saline solution with pepstatin (5 μg/ml), leupeptin (5 μg/ml), and aprotinin (2 μg/ml) as protease inhibitors. The livers were then transferred into a beaker, on ice, containing the homogenization buffer (2 M sucrose, 10 mM Hepes, pH 7.6, 25 mM KCl, 0.15 mM spermine, 0.5 mM spermidine, 1 mM EDTA, 10% glycerol, 0.5 mM dithiothreitol) and minced with scissors. After processing in a Dounce apparatus in fresh buffer on ice, the homogenates were layered on 2 M sucrose cushions and centrifuged at 80,000 *g* for 35 min at 0 °C. The nuclear pellets were then rinsed in a buffer containing 10 mM of Tris, pH 7.4, 10 mM of NaCl, 3 mM of $MgCl_2$, resuspended in a 20 mM Hepes, pH 7.9, 0.4 M NaCl, 1 mM EDTA, 1 mM EGTA, 1 mM dithiothreitol buffer and incubated 15 min on ice. After spinning 5 min at 10,000 rpm, aliquots of the supernatants were stored at −80 °C. The protein content was determined as described by Bradford, using bovine serum albumin as a standard.

3.7. Statistical analysis

Data were statistically analyzed by performing a nonparametric Mann–Whitney test using GraphPad Prism to compare experimental groups (v. 6.00 for Windows, San Diego, CA, USA). Data were expressed as mean < remove picture pageno 5> standard error of the mean (SEM) and considered significant at $P < 0.05$.

4. Results

4.1. Body and liver weights, body fat accumulation and biochemical parameters

The administration of a high-carbohydrate diet for 6 months resulted in significant increases in the final body, liver and abdominal fat weights compared with those in the gerbils from the control group (Table 3). The liver and fat indices increased 1.08 and 2.5 times, respectively, compared to the control diet, after a 24-week HC diet. The HCD group showed higher plasma concentrations of triglycerides ($P < 0.001$) and total cholesterol ($P < 0.05$). However, the mean plasma HDL cholesterol and LDL cholesterol levels were not statistically different between the two groups. Plasma glucose was not modified in experimental gerbils ($P = 0.123$), whereas plasma insulin level and HOMA-IR index were significantly increased ($P < 0.05$) with the HCD compared to the control diet (Table 3). The 24-week feeding of HCD to gerbils did not significantly affect ALT and AST activities (markers of liver function) (Table 3).

4.2. Liver TG and cholesterol levels

The liver TG and TC levels are shown in Table 3. HCD feeding significantly increased the hepatic TG levels (188.4 ± 26.20 mg/g) compared with the control group (82.97 ± 12.07 mg/g; $P < 0.01$). The hepatic TC content in the HCD group was increased two times compared to control animals.

Table 3
Physiological and plasma parameters in control and HCD gerbils after 24 weeks of treatment.

	Control ($n = 6$)	Experimental ($n = 6$)
Body weight (g)	27.68 ± 0.88	31.43 ± 0.70**
Fat pads (mesenteric, genital and perirenal) (g)	0.49 ± 0.03	1.35 ± 0.15***
Fat to body weight ratio (%)	1.76 ± 0.10	4.35 ± 0.57**
Liver weight (g)	0.98 ± 0.005	1.19 ± 0.005*
Liver to body weight ratio (%)	3.51 ± 0.21	3.79 ± 0.11
Hepatic triglycerides (mg/g liver)	82.97 ± 12.07	188.4 ± 26.20**
Hepatic total cholesterol (mg/g liver)	41.45 ± 8.20	86.86 ± 3.85***
Plasma triglycerides (mg/dl)	93.91 ± 10.04	208 .7 ± 18.48***
Plasma total cholesterol (mg/dl)	103.1 ± 7.05	136.8 ± 9.03*
Plasma HDL-c (mg/dl)	57.07 ± 3.55	51.52 ± 5.20
Plasma LDL-c (mg/dl)	28.81 ± 8.95	42.33 ± 8.14
Plasma glucose (mg/dl)	94.74 ± 3.73	107.8 ± 6.78
Plasma insulin (mU/mL)	48.38 ± 2.21	183.9 ± 47.26*
HOMA-IR index	11.34 ± 0.79	48.91 ± 12.78*
ASAT (U/l)	32.08 ± 7.02	56.84 ± 25.71
ALAT (U/l)	18.95 ± 2.68	24.78 ± 4.17

Data are expressed as means ± SEM.
* $P < 0.05$.
** $P < 0.01$.
*** $P < 0.001$ versus the control group.

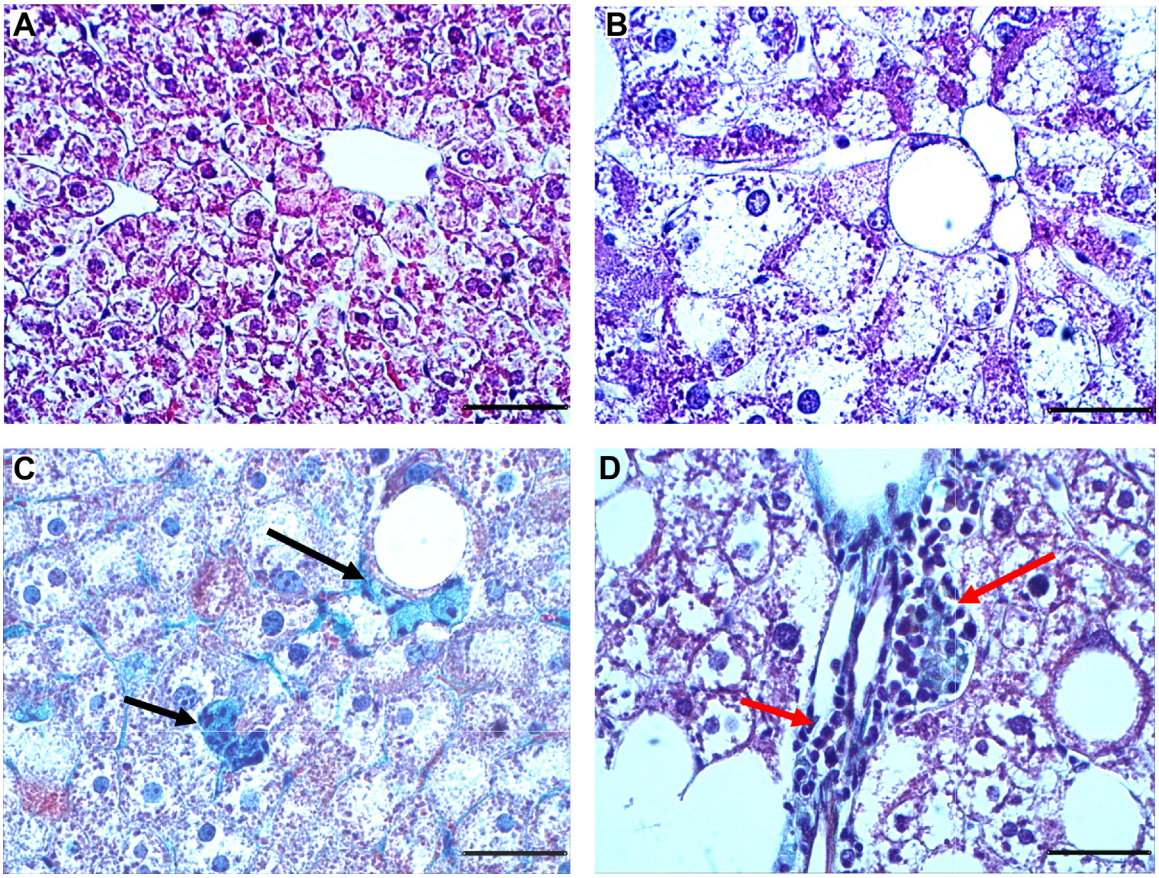

Fig. 1. Representative Masson Trichrome stained liver sections from gerbils fed with normal diet (A) or high carbohydrate diet (B–D) during 24 weeks. Trichrome Masson staining was performed to detect fibrotic areas (in green, indicated by arrows). Sections were observed at 400-fold magnification (scale bars: 50 μm).

4.3. Histological analysis of the liver tissues

Representative photomicrographs of liver sections are described in Fig. 1. Liver sections of control animals showed a normal liver architecture formed of hepatic lobules. Briefly, each lobule is made up of radialing plates. Strands of cells form a network around a central vein (Fig. 1A). The histological examination of liver tissue of gerbils submitted to the HC diet revealed variable changes. These changes were evidenced by a marked micro and macro steatosis characterizing the NAFLD status (Fig. 1B). Trichrome staining showed a marked collagen deposition within the pericellular space at sites where fatty degeneration of hepatocytes occurred (Fig. 1C). Also, marked mononuclear cell infiltrates in the portal system space (red arrows) were observed (Fig. 1D).

4.4. Lipid peroxidation of the liver

As shown in Fig. 2A, the level of malondialdehyde (MDA), an index of lipid peroxidation in liver homogenates was significantly increased by 67% in the HCD group ($P < 0.05$) compared to the control group.

4.5. Activities of antioxidant enzymes in liver tissue

The effect of a long-term administration of HCD on activities of liver antioxidant enzymes is depicted in Fig. 2(B–E). GSH (reduced glutathione) levels were statistically significantly lower in the HCD group than in the control group (Fig. 2B). SOD (superoxide dismutase) activities did not yield statistically significant differences due to the large variability observed (HCD: (0.600 ± 0.129 U/mg protein) vs. (0.914 ± 0.331 U/mg protein) in control animals). As illustrated in Fig. 2A and B, the GST (glutathione-*S*-transferase) and CAT (catalase) activities were unchanged between these two groups.

4.6. Hepatic gene expression in gerbils

4.6.1. mRNA expression of SREBP1c. ACC and FAS

Sterol regulatory element-binding protein-1 (SREBP-1) is a nuclear transcription factor that transcriptionally activates nearly all the genes involved in *de novo* lipogenesis [23]. Acetyl-CoA carboxylase (ACC) and fatty acid synthase (FAS) are important downstream target genes of SREBP-1 and are the rate-limiting enzymes of

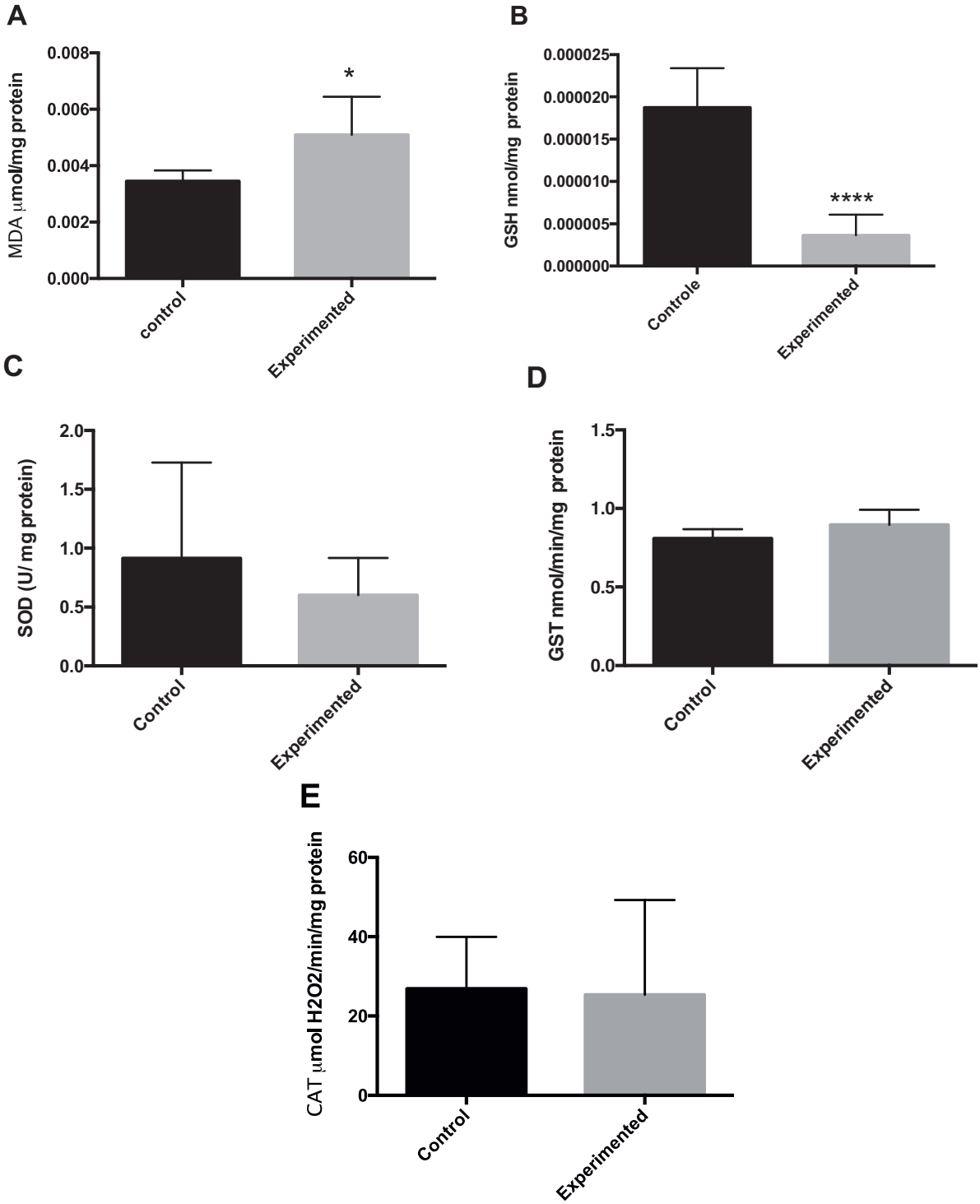

Fig. 2. Oxidative stress in liver tissue. The intrahepatic contents in MDA (A), GSH (B), SOD (C), GST (D) and CAT (E) were respectively measured in frozen liver homogenate of control or treated gerbils. * $P < 0.05$. **** $P < 0.0001$ versus control group.

palmitate formation. Compared with controls, HCD feeding alone significantly up-regulated the hepatic mRNA expression of SREBP1-c ($P < 0.01$), FAS ($P < 0.001$) and ACC ($P < 0.01$) (Fig. 3A–C).

4.6.2. mRNA expression of SREBP2, HMG CoA synthase and HMG CoA reductase

SREBP-2 preferentially regulates target genes involved in cholesterol biosynthesis and uptake in the liver, such as

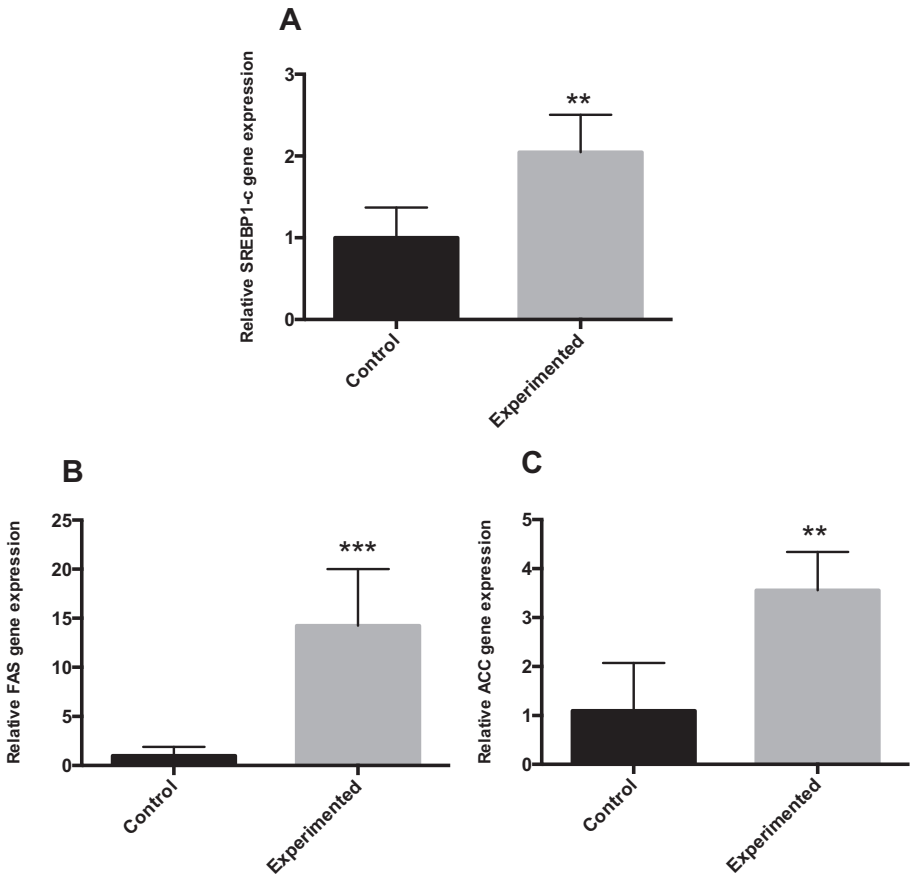

Fig. 3. mRNA expression for genes involved in fatty acid synthesis in the liver of gerbils fed normal diet or high carbohydrate diet for 24 weeks. ** $P < 0.01$. *** $P < 0.001$ vs. the corresponding values in control gerbils.

3-hydroxy-3-methylglutaryl-CoA synthase (HMGCS) and 3-hydroxy-3-methylglutaryl-CoA reductase (HMGCR) [24]. The mRNA expressions of SREBP-2 and HMG CoA synthase were significantly increased in HCD gerbils as compared to controls (Fig. 4A–B). However, HMGCoA reductase mRNA expression was not significantly different between the groups, due to the large variability observed, but tended to increase as compared to controls (Fig. 4C).

4.6.3. mRNA expression of α-SMA, Col1A1 and TGF-β

Our results show that mRNA gene expression for α-SMA (α-smooth muscle actin, a gene related to stellate cell activation) was approximatively two-fold higher in HCD group compared to control group ($P < 0.05$). Similarly, the hepatic mRNA expression of Col1A1 (collagen 1A1) was up-regulated (1.5-fold) in HCD group compared to control group (Fig. 5B). However, liver expression of TGF-β (transforming growth factor) remained unchanged between the two groups (Fig. 5C).

4.6.4. mRNA expression of GRP78 and ORP150

Abnormal endoplasmic reticulum (ER) stress contributes substantially to hepatocyte cell death during altered lipid metabolism [25]. To investigate whether ER stress was associated with the pathogenesis of hepatic steatosis, we studied GRP78 (glucose-regulated protein 78) by RT-PCR. GRP78 acts as an apoptotic regulator by protecting or promoting cell death during ER stress [26]. The RT-PCR results indicated that the GRP78 mRNA expression level was elevated in the experiment group, compared with the corresponding control groups (+ 44 %) (Fig. 6A). The 150-kDa oxygen-regulated protein (ORP150) is an anti-apoptotic ER resident chaperone that exerts a protective effect against ER stress-dependent apoptosis [27]. As shown in Fig. 6B, ORP150 mRNA expression was significantly increased in the HCD group compared with the control group ($P < 0.05$).

5. Discussion

In this study, after 24 weeks of feeding with HCD (dates and barley), gerbils exhibited increased body weight, visceral fat mass, visceral fat/body weight ratio, and liver/body weight ratio when compared with control animals. HCD treatment also caused significant increments in the plasma TC and TG levels, elevated hepatic TG and TC contents, and marked lipid droplet deposition in the liver sections, which are consistent with signs of fatty liver. At

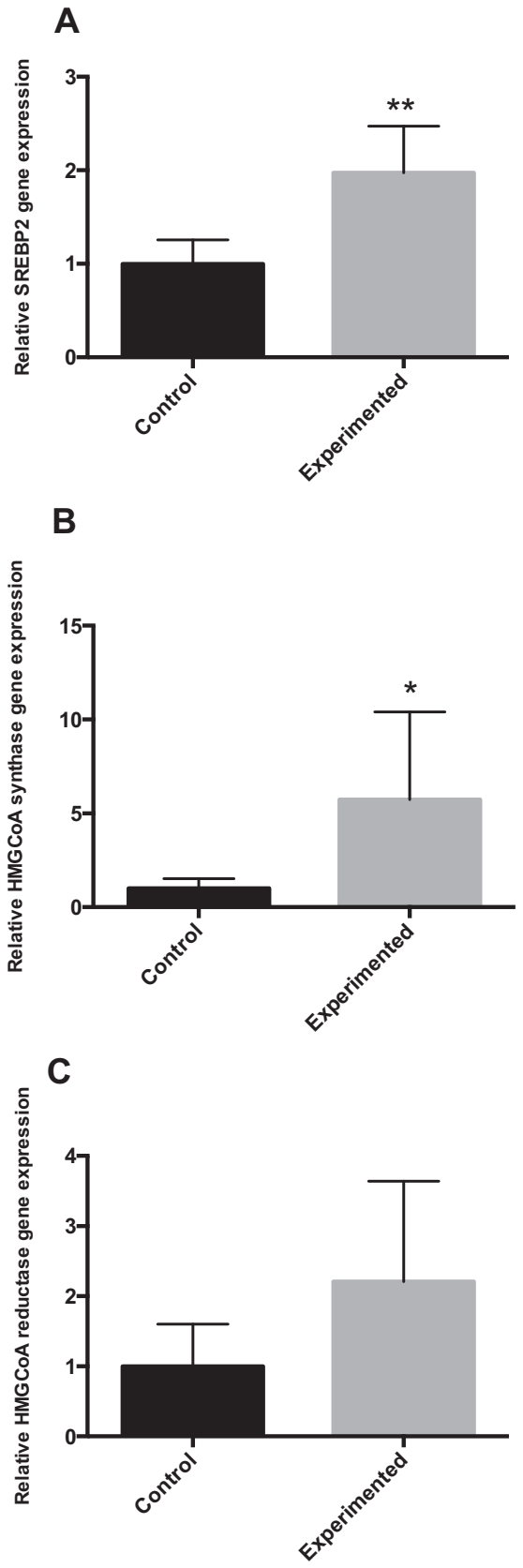

this time, the liver enzymes (ALT and AST) levels were normal, suggesting that the presence of NASH does not necessarily correlate with higher levels of these liver transaminases. Indeed, ALT levels are persistently normal in more than one half of the patients with NAFLD and biopsy proven NASH [28]. It is interesting to note that after 24 weeks of dietary treatment, the HCD group exhibited no significant changes (but a 14% increased trend) in the plasma glucose level. In addition, HCD induced hyperinsulinemia and insulin resistance (confirmed by HOMA-IR calculation).

Body fat distribution appears to be even more important than the total amount of adipose tissue, and the visceral fat mass is strongly linked to insulin resistance and NAFLD [29]. Visceral fat-released FFAs are transported to the liver by the portal vein and may contribute to hepatic steatosis, production of triglyceride rich VLDL, and elevated β-oxidation [30].

A large body of evidence supports a complex interaction between NAFLD and insulin resistance [31]. Some studies have suggested that the abdominal adipose tissue plays an important role in the development of insulin resistance [32]. Furthermore, visceral adipose tissue (VAT), a harmful fat deposit, has been considered to induce liver insulin resistance and further induce systemic insulin resistance [33].

This study demonstrates that a high-carbohydrate diet was able to induce obesity-related NAFLD in our experimental model. Animal models in which NAFLD was induced by simple carbohydrate-rich diets (usually fructose) are less numerous, and in most of them only hepatic steatosis was observed [34,35]. Hyperinsulinemia led to increased hepatic synthesis of fatty acids, triglyceride accumulation in the hepatocytes, with subsequent steatosis. Several *in vivo* and *in vitro* studies have indicated that hepatic TG deposition may not be harmful; rather, it may represent a protective mechanism against FFA-induced lipotoxic liver injury by storing FFAs in the form of TGs [36].

Increased calorie intake, especially refined sugar and fructose, correlates with increases in dyslipidemia, IR, and nonalcoholic fatty liver disease (NAFLD) [37]. NAFLD is the first step in the hepatic diseases that can evolve into steatohepatitis (NASH), with inflammatory infiltration resulting in cirrhosis, and even hepatocarcinomas [38].

Epidemiologic studies suggested that a diet high in refined carbohydrates (HCD) (50–65% of energy from carbohydrates, high glycemic index, and low in fiber) could promote NAFLD progression [39]. Our work demonstrates that gerbils fed a high glycemic index diet (GI for dates is 70) for 24 weeks had greater hepatic TGs and adiposity than gerbils fed a low glycemic index diet. Our results fit with those of Scribner et al. [40]. In addition, several experiments showed that the high-glycemic index

Fig. 4. mRNA expression of SREBP2 and SREBP2 (HMGCoA synthase, HMGCoA reductase) target gene involved in cholesterol metabolism in the liver of gerbils fed with normal diet or high-carbohydrate diet for 24 weeks. * $P < 0.05$. ** $P < 0.01$ vs. the corresponding values in control gerbils.

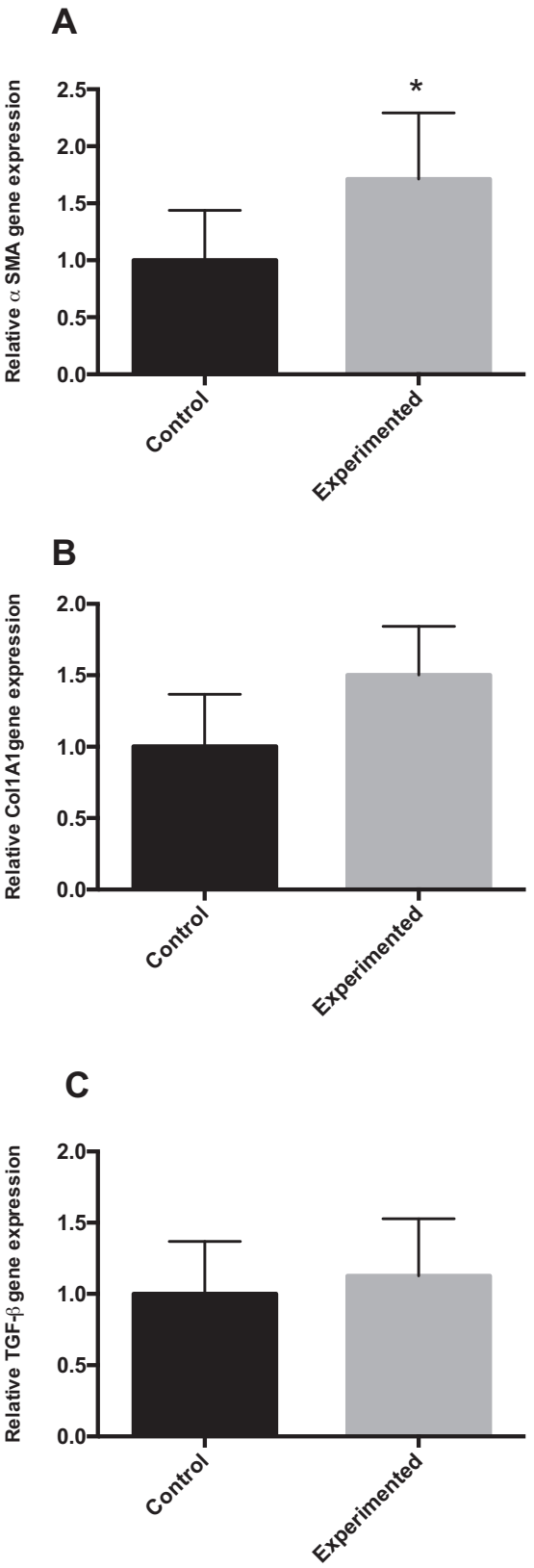

Fig. 5. mRNA expression for genes related to hepatic fibrosis in the liver of gerbils fed with normal diet or high-carbohydrate diet for 24 weeks. * $P < 0.05$ vs. the corresponding value in control gerbils.

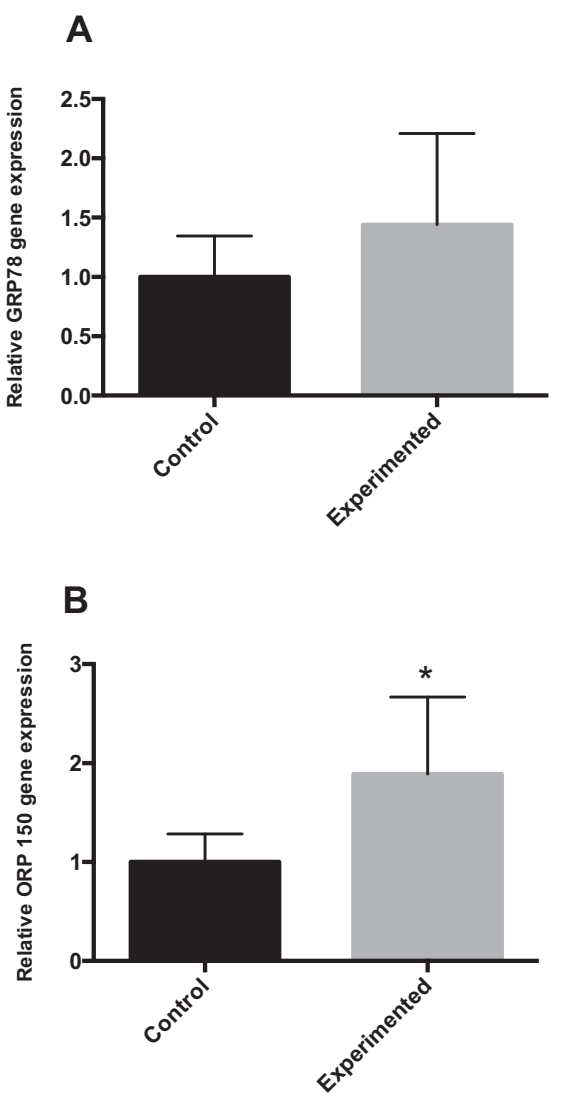

Fig. 6. Expression of ER stress markers in the livers of control and experimental gerbils. * $P < 0.05$ vs. the corresponding values in control gerbils.

carbohydrate has a close relationship with obesity, IR, and increased plasma and hepatic TGs [40]. The grade of hepatic steatosis seems to be associated with the glycemic index of the diet, regardless of total energy or carbohydrate intake [39]. The underlying mechanism is not fully elucidated, but some hypotheses have been proposed. Foods with high glycemic indices enhance the hepatic influx of glucose. The excess of hepatic glucose exceeds the ability of glycogen production; therefore, this carbohydrate will be used for the synthesis of new TG through DNL within the hepatocytes. An elevated-glycemic index food might augment oxidative stress, which can contribute to NASH development [41].

Similarly, Maersk et al. [42] found that a daily intake of 1 L of a sucrose-sweetened soft drink for six months increased liver lipids in overweight participants compared with the intake of the same amount of milk, diet cola, or

water. Carbohydrate-induced accumulation of fat in the liver can lead to nonalcoholic fatty liver disease (NAFLD) [43].

The composition of diet and especially the amount of glucose/starch may influence the health effects of fructose. As fructose is present with glucose in most food products, it is more practical and relevant to look at the effects of fructose and glucose together than at the effects of fructose alone. A larger increase in DNL after eating fructose and glucose together (50:50 glucose:fructose) rather than the same amount of pure glucose has been shown [44]. Eating glucose with fructose is likely to affect fructose's health effects by stimulating the flow of fructose to DNL [45]. This effect could be due to both increased absorption capacity for fructose when co-ingested with glucose and therefore greater availability of fructose carbon atoms going towards DNL and increased blood insulin levels when glucose is present in the diet. Insulin stimulates DNL directly and indirectly by inhibiting other important metabolic pathways for fructose, such as gluconeogenesis.

In the present study, HCD-fed gerbil had severe hepatic steatosis. This HCD-induced elevated steatosis was associated with the significant upregulation of DNL genes, including FAS (an enzyme that catalyzes long-chain fatty acid biosynthesis through the condensation of acetyl-CoA and malonyl-CoA and ACC, as well as SREBP (a key regulator of fatty acid synthesis in the liver gene expression). This evidence is consistent with previous in vivo studies and clinical observations that HCD-induced NAFLD was associated with elevated hepatic DNL [39]. Donnelly et al. [4] observed that patients with NAFLD have elevated fasting DNL compared with healthy individuals. Altering dietary macronutrient contents can induce differential metabolic consequences in the liver [46]. Excessive dietary carbohydrates induced glucose conversion to FA by DNL [46]. It is important to note that diets rich in complex carbohydrates and fibers did not induce clinical DNL in humans, suggesting a potential interaction between digestibility/structure of carbohydrates and DNL [47]. The deleterious effect of our diet is attributed to dry dates that contain essentially simple sugars.

The liver is the major organ involved in cholesterol metabolism. Sterol regulatory element-binding protein-2 (SREBP-2) promotes the expression of target genes involved in cholesterol biosynthesis and uptake in the liver, such as 3-hydroxy-3-methylglutaryl-CoA synthase (HMGCS) and 3-hydroxy-3-methylglutaryl-CoA reductase (HMGCR) [24]. The data from the present investigation (Fig. 4) showed that the SREBP-2 precursor and nuclear active forms as well as the HMGCR and HMGCS target genes were significantly up-regulated by HCD in gerbil.

Previous research has shown that a fatty liver induced by a high saturated fat diet shows signs of endoplasmic reticulum (ER) stress in a rodent model [48]. The endoplasmic reticulum is an important organelle responsible for protein synthesis, folding, assembly and transport in eukaryotic cells. GRP78 is a member of the HSP70 family abundant in the lumen of ER, and plays important roles as a molecular chaperone that removes misfolded proteins in ER lumen. Overexpression of GRP78 has been shown to increase ER stress resistance and to have beneficial effects in several cell types [49]. In addition, the survival response activates genes that encode ER-residing chaperones such as GRP78/Bip, which uses energy derived from ATP hydrolysis to prevent the aggregation of ER proteins, and is considered the classical marker of UPR activation.

To confirm the involvement of ER in fatty liver developed in our experimented gerbils, we studied GPR78 and ORP150 by quantitative RT-PCR, and the data in Fig. 5 show that GRP78 moderately increased in *G. gerbillus* liver. It was demonstrated that obesity is associated with the induction of ER stress predominantly in the liver and adipose tissues [50]. Previous research has shown that fatty liver induced by a high sucrose diet and high saturated fat diet shows clear ER stress events in a rodent model [48].

In the current study, we observed a coordinated transcriptional upregulation of lipogenesis genes together with ER stress. Lipid accumulation and lipotoxicity are known to positively regulate the ER stress response through a cycle that leads to further toxic insults upon the liver [51].

Abnormal ER stress contributes substantially to hepatocyte cell death during altered lipid metabolism [24]. Thus, modulation of hepatic ER stress becomes crucial in the understanding of the extent of its contribution to the pathogenesis of various hepatic disorders. Induction of ORP150 exhibits protective roles in the prevention of ER stress [27] and dysregulation of calcium homeostasis and apoptosis. Our work showed that the levels of ORP150 in the liver of control gerbils were significantly greater compared with that of experimented gerbils (Fig. 5B), which supports the speculation that ORP150 expression could be beneficial under the local challenging conditions of ER stress.

The induction of ORP150 mediates the amelioration of hepatic ER stress and apoptosis by AMPK *in vitro* and *in vivo*. [52] Collectively, these results indicate that chronic HC diet altered, at least partially, endoplasmic reticulum functions and induced stress conditions.

Collagen 1A1 (Col1A1) is the major hepatic collagen subtype associated with NASH in rodents and humans [53]. HC-feeding for 24 weeks greatly elevated biochemical and histological markers of fibrosis. The fibrotic status of the liver is governed by a balance between extracellular matrix (ECM) deposition and turnover. The biochemical (expression of αSMA) and histological evidence of fibrosis (Fig. 1) in HC fed gerbils provide clear evidence that the rate of collagen production exceeds that of its degradation.

Although it has been widely proposed that stellate cells are the main contributor to ECM deposits in the liver, it is possible that other cell types are involved [54]. MMPs are a family of zinc-dependent proteinases that are responsible for the degradation of ECM proteins. MMP dysregulation has been implicated in the pathophysiology of obesity and diabetes.

Overwhelming evidence indicates that the perisinusoidal hepatic stellate cells (HSCs) are the major source of liver fibrosis of any etiology [55]. During liver injury, HSCs

transdifferentiate from their quiescent physiologic to the fibrogenic phenotype. Such a transformation is induced by inflammatory mediators (e.g., TNFα) and reactive oxygen species and apoptotic bodies arising from dying hepatocytes, and activated HSCs are characterized by expression of αSMA, a marker not found in quiescent HSCs [56,57].

Activation of HSCs is further characterized by the overexpression of α-SMA, MMP-2, and MMP-9 [58]. Although the role of HSC activation in nonalcoholic fatty liver disease (NAFLD) has not been completely clarified, several studies have reported increased HSC activation in nonalcoholic steatohepatitis (NASH) [59].

Several studies have demonstrated that insulin resistance is associated with advanced stages of fibrosis in NAFLD [60]. Because insulin promotes HSC activation and insulin sensitizers can attenuate hepatic fibrosis in NASH, it has been suggested that insulin resistance plays an important role in NASH-related fibrogenesis [61]. It is understood that oxidative stress induces the activation of HSCs in NASH [62].

In addition to liver fibrosis, it is well-established that oxidative stress also is very important in the development and progression of NASH. It has been shown that chronic oxidative stress, generated through the oxidation of cytotoxic free fatty acids, may lead to cytokine upregulation and depletion of hepatic antioxidant levels [63]. In addition, enhanced lipid peroxidation leads to the generation of reactive by-products, such as MDA, which have been shown to further stimulate cytokine production [64]. In the current study, there was a significant decrease in GSH content and SOD activity in HC-fed gerbils, and a significant increase in MDA levels. These findings are in agreement with those of Leclercq [65], who reported that diets with high amounts of simple carbohydrates induce hypertriglyceridemia, resulting in a reduction of the antioxidant reserves [65].

Most previous studies reported alterations in the expression and activity of antioxidant enzymes in the liver of fructose-fed rodents, although the course of these alterations varied largely. Some authors observed that a fructose-rich diet reduced the antioxidant capacity and caused oxidative damages in the liver [66], whereas others reported the absence of oxidative stress [67] or adaptation to modest oxidative stress [68] in fructose-fed rats. Alternatively, Girard et al. [69] noticed that a fructose-rich diet enhanced the total antioxidant capacity of the liver.

6. Conclusion

In summary, the present study demonstrates that a long-term (24-week) consumption of a high-carbohydrate diet induces adiposity, insulin resistance, up-regulation of *de novo* lipogenesis, ER stress, oxidative stress, and finally fatty liver. Altogether, these results suggest that *G. gerbillus* represents a valuable natural model for human diet-induced metabolic disorders and NAFLD.

Disclosure of interest

The authors declare that they have no competing interest.

Acknowledgments

We would like to thank Professor Ahmed Menad for her help and collaboration.

References

[1] A. Tonjes, M. Bluher, M. Stumvoll, Retinol-binding protein 4 and new adipocytokines in nonalcoholic fatty liver disease, Curr. Pharm. Design. 16 (2010) 1921–1928.
[2] R. Loomba, A.J. Sanyal, The global NAFLD epidemic, Nat. Rev. Gastroenterol. Hepatol. 10 (2013) 686–690.
[3] S.K. Erickson, Nonalcoholic fatty liver disease, J. Lipid. Res. 50 (2009) S412–S416.
[4] K.L. Donnelly, C.I. Smith, S.J. Schwarzenberg, J. Jessurun, M.D. Boldt, E.J. Parks, Sources of fatty acids stored in liver and secreted via lipoproteins in patients with nonalcoholic fatty liver disease, J. Clin. Invest. 115 (2005) 1343–1351.
[5] C. Postic, J. Girard, Contribution of de novo fatty acid synthesis to hepatic steatosis and insulin resistance: lessons from genetically engineered mice, J. Clin. Invest. 118 (2008) 829–838.
[6] K. Kantartzis, F. Schick, H.U. Haring, N. Stefan, Environmental and genetic determinants of fatty liver in humans, Dig. Dis. 28 (2010) 169–178.
[7] I. Shimomura, H. Shimano, B.S. Korn, Y. Bashmakov, J.D. Horton, Nuclear sterol regulatory element-binding proteins activate genes responsible for the entire program of unsaturated fatty acid biosynthesis in transgenic mouse liver, J. Biol. Chem. 273 (1998) 35299–35306.
[8] P. Ferre, F. Foufelle, SREBP-1c transcription factor and lipid homeostasis: clinical perspective, Horm. Res. 68 (2007) 72–82.
[9] P. Ferre, F. Foufelle, Hepatic steatosis: a role for de novo lipogenesis and the transcription factor SREBP-1c, Diabetes. Obes. Metab. 12 (2010) 83–92.
[10] P. Puri, F. Mirshahi, O. Cheung, R. Natarajan, J.W. Maher, J.M. Kellum, A.J. Sanyal, Activation and dysregulation of the unfolded protein response in nonalcoholic fatty liver disease, Gastroenterology 134 (2008) 568–576.
[11] D.L. Fang, Y. Wan, W. Shen, J. Cao, Z.X. Sun, H.H. Yu, Q. Zhang, W.H. Cheng, J. Chen, B. Ning, Endoplasmic reticulum stress leads to lipid accumulation through upregulation of SREBP-1c in normal hepatic and hepatoma cells, Mol. Cell. Biochem. 381 (2013) 127–137.
[12] Q.M. Anstee, R.D. Goldin, Mouse models in nonalcoholic fatty liver disease and steatohepatitis research, Int. J. Exp. Pathol. 1 (2006) 11–16.
[13] Y. Takahashi, Y. Soejima, T. Fukusato, Animal models of nonalcoholic fatty liver disease/nonalcoholic steatohepatitis, World. J. Gastroenterol. 18 (2012) 2300–2308.
[14] J. Folch, M. Lees, G.H. Sloane Stanley, A simple method for the isolation and purification of total lipides from animal tissues, J. Biol. Chem. 226 (1957) 497–509.
[15] H. Ohkawa, N. Ohishi, K. Yagi, Assay for lipid peroxides in animal tissues by thiobarbituric acid reaction, Anal. Biochem. 95 (1979) 351–358.
[16] S. Marklund, G. Marklund, Involvement of the superoxide anion radical in the autoxidation of pyrogallol and a convenient assay for superoxide dismutase, Eur. J. Biochem. 16 (1974) 469–474.
[17] H. Aebi, Catalase in vitro, Methods. Enzymol. 105 (1984) 121–126.
[18] W.H. Habig, M.J. Pabst, W.B. Jakoby, Glutathione-S-transferase. The first step in mercapturic acid formation, J. Biol. Chem 249 (1974) 7130–7139.
[19] G.L. Ellman, Tissue sulfhydryl groups, Arch. Biochem. Biophys. 82 (1959) 70–77.
[20] M.M. Bradford, A rapid and sensitive method for quantization of microgram quantities of protein utilizing the principle of protein-dye binding, Anal. Biochem. 72 (1976) 248–254.
[21] P. Chomczynski, N. Sacchi, Single-step method of RNA isolation by acid guanidinium thiocyanate-phenol-chloroform extraction, Anal. Biochem. 162 (1987) 156–159.
[22] A. Bobard, I. Hainault, P. Ferré, F. Foufelle, P. Bossard, Differential regulation of sterol regulatory element-binding protein 1c transcriptional activity by insulin and liver X receptor during liver development, J. Biol. Chem. 280 (2005) 199–206.
[23] K. Wouters, P.J. van Gorp, V. Bieghs, M.J. Gijbels, H. Duimel, D. Lütjohann, A. Kerksiek, N. Maeda, B. Staels, M.V. Bilsen, R. Shiri-Sverdlov, M.H. Hofker, Dietary cholesterol rather than liver steatosis leads to hepatic infammation in hyperlipidemic mouse models of nonalcoholic steatohepatitis, Hepatology 48 (2008) 474–486.
[24] M.S. Brown, J.L. Goldstein, The SREBP pathway: regulation of cholesterol metabolism by proteolysis of a membrane-bound transcription factor, Cell 89 (1997) 331–340.

[25] M. Flamment, H.L. Kammoun, I. Hainault, P. Ferré, F. Foufelle, Endoplasmic reticulum stress: a new actor in the development of hepatic steatosis, Curr. Opin. Lipidol. 21 (2010) 239–246.
[26] J. Li, M. Ni, B. Lee, E. Barron, D.R. Hinton, A.S. Lee, The unfolded protein response regulator GRP78/BiP is required for endoplasmic reticulum integrity and stress-induced autophagy in mammalian cells, Cell. Death. Differ. 15 (2008) 1460–1471.
[27] M. Sanson, N. Auge, C. Vindis, C. Muller, Y. Bando, J.C. Thiers, M.A. Marachet, K. Zarkovic, Y. Sawa, R. Salvayre, A. Negre-Salvayre, Oxidized low-density lipoproteins trigger endoplasmic reticulum stress in vascular cells: prevention by oxygen-regulated protein 150 expression, Circ. Res. 104 (2009) 328–336.
[28] A.L. Fracanzani, L. Valenti, E. Bugianesi, M. Andreoletti, A. Colli, E. Vanni, C. Bertelli, E. Fatta, D. Bignamini, G. marchesini, S. Fargion, Risk of severe liver disease in nonalcoholic fatty liver disease with normal aminotransferase levels: a role for insulin resistance and diabetes, Hepatology 48 (2008) 792–798.
[29] G. Calamita, P. Portincasa, Present and future therapeutic strategies in nonalcoholic fatty liver disease, Expert. Opin. Ther Targets 11 (2007) 1231–1249.
[30] M.D. Jensen, Role of body fat distribution and the metabolic complications of obesity, J. Clin. Endocrinol. Metab. 93 (2008) S57–S63.
[31] H.H. Nam, D.W. Jun, H.J. Jeon, J.S. Lee, W.K. Saeed, E.K. Kim, Osthol attenuates hepatic steatosis via decreased triglyceride synthesis not by insulin resistance, World. J. Gastroenterol. 20 (2014) 11753–11761.
[32] M. Mamtani, H. Kulkarni, T.D. Dyer, L. Almasy, M.C. Mahaney, R. Duggirala, A.G. Comuzzie, J. Blangero, J.E. Curran, Waist circumference independently associates with the risk of insulin resistance and type 2 diabetes in Mexican American families, PLoS. One. 8 (2013) 153–159.
[33] P. Patel, N. Abate, Body fat distribution and insulin resistance, Nutrients 5 (2013) 2019–2027.
[34] R. Kohli, M. Kirby, S.A. Xanthakos, S. Softic, A.E. Feldstein, V. Saxena, P.H. Tang, L. Miles, M.V. Miles, W.F. Balistreri, S.C. Woods, R.J. Seeley, High-fructose, medium chain trans fat diet induces liver fibrosis and elevatesplasma coenzyme Q9 in a novel murine model of obesity and nonalcoholic steatohepatitis, Hepatology 52 (2010) 934–944.
[35] F. Armutcu, O. Coskun, A. Gürel, M. Kanter, M. Can, F. Ucar, M. Unalacak, Thymosin alpha 1 attenuates lipid peroxidation and improves fructose-induced steatohepatitis in rats, Clin. Biochem. 38 (2005) 540–547.
[36] L.L. Listenberger, X. Han, S.E. Lewis, S. Cases, R.V. Farese, D.S. Ory, J.E. Schaffer, Triglyceride accumulation protects against fatty acid-induced lipotoxicity, Proc. Natl. Acad. Sci. USA 100 (2003) 3077–3082.
[37] K. Nomura, T. Yamanouchi, The role of fructose-enriched diets in mechanisms of nonalcoholic fatty liver disease, J. Nutr. Biochem. 23 (2012) 203–208.
[38] L. Tappy, K.A. Le, C. Tran, N. Paquot, Fructose and metabolic diseases: new findings. New questions, Nutrition 26 (2010) 1044–1049.
[39] S. Valtueña, N. Pellegrini, D. Ardigò, D. Del Rio, F. Numeroso, F. Scazzina, L. Monti, I. Zavaroni, F. Brighenti, Dietary glycemic index and liver steatosis, Am. J. Clin. Nutr. 84 (2006) 136–142 [quiz 268–9].
[40] K.B. Scribner, D.B. Pawlak, D.S. Ludwig, Hepatic steatosis and increased adiposity in mice consuming rapidly vs. slowly absorbed carbohydrate, Obesity (Silver Spring) 15 (2007) 2190–2199.
[41] Y. Hu, G. Block, E.P. Norkus, J.D. Morrow, M. Dietrich, M. Hudes, Relations of glycemic index and glycemic load with plasma oxidative stress markers, Am. J. Clin. Nutr. 84 (2006) 70–76.
[42] M. Maersk, A. Belza, H. Stødkilde-Jørgensen, S. Ringgaard, S. Chabanova, S. Thomsen, S.B. Pedersen, A. Astrupe, B. Richeisen, Sucrose sweetened beverages increase fat storage in the liver, muscle, and visceral fat depot: a 6-morandomized intervention study, Am. J. Clin. Nutr. 95 (2012) 283–289.
[43] K.A. Page, O. Chan, J. Aroraetal, Effects of fructose vs glucose on regional cerebral blood flow in brain regions involved with appetite and reward pathways, JAMA 309 (2013) 63–70.
[44] E.J. Parks, L.E. Skokan, M.T. Timlin, C.S. Dingfelder, Dietary sugars stimulate fatty acid synthesis in adults, J. Nutr. 138 (2008) 1039–1046.
[45] F. Eytaz, S. de Giorgi, L. Hodson, N. Stefanoni, V. rey, P. Schnitter, V. Giusti, L. Tappy, Metabolic fate of fructose ingested with and without glucose in a mixed meal, Nutrients 6 (2014) 2632–2649.
[46] S. Solga, A.R. Alkhuraishe, J.M. Clark, M. Torbenson, A. Greenwald, A.M. Diehl, T. Magnuson, Dietary composition and nonalcoholic fatty liver disease, Dig. Dis. Sci. 49 (2004) 1578–1583.
[47] L.C. Hudgins, M.K. Hellerstein, C.E. Seidman, R.A. Neese, J.D. Tremaroli, J. Hirsch, Relationship between carbohydrate-induced hypertriglyceridemia and fatty acid synthesis in lean and obese subjects, J. Lipid. Res. 41 (2000) 595–604.
[48] D. Wang, Y. Wei, M.J. Pagliassotti, Saturated fatty acids promote endoplasmic reticulum stress and liver injury in rats with hepatic steatosis, Endocrinol. 147 (2006) 943–951.
[49] E.G. Lai, M.B. Bikopoulos, M. Wheeler, A. Rozakis-Adcock, A. Volchuk, Differential activation of ER stress and apoptosis in response to chronically elevated free fatty acids in pancreatic beta-cells, Am. J. Physiol. Endocrinol. Metab. 294 (2008) E540–E550.
[50] U. Ozcan, Q. Cao, E. Yilmaz, A.H. Lee, N.N. Lwakoshil, E. özdelen, G. Tunkman, C. Görgun, L.H. Glimcher, G.S. Hotamisligil, Endoplasmic reticulum stress links obesity, insulin action, and type 2 diabetes, Science 306 (2004) 457–461.
[51] L.H. Glimcher, A.H. Lee, From sugar to fat: how the transcription factor XBP1 regulates hepatic lipogenesis, Ann. NY. Acad. Sci. 1173 (2009) E2–E9.
[52] Y. Wang, W. Wu, D. Li, D. Wang, X. Wang, X. Feng, M. Xia, Involvement of oxygen-regulated protein 150 in AMP-activated protein kinase-mediated alleviation of lipid-induced endoplasmic reticulum stress, J. Biol. Chem. 286 (2011) 11119–11131.
[53] J.R. Clapper, M.D. Hendricks, G. Gu, C. Wittmer, C.S. Dolman, J. Herich, J. Athanasio, C. Villescaz, S.S. Soumitra, S. Ghosh, J.S. Heilig, C. Lowe, J.D. Roth, Diet-induced mouse model of fatty liver disease and nonalcoholic steatohepatitis reflecting clinical disease progression and methods of assessment, Am. J. Physiol Gastrointest. Liver. Physiol. 305 (2013) G483–G495.
[54] R. Bataller, D.A. Brenner, Hepatic stellate cells as a target for the treatment of liver fibrosis, Semin. Liver Dis. 21 (2001) 437–451.
[55] K.M. Thrailkill, R. Clay Bunn, J.L. Fowlkes, Matrix metalloproteinases: their potential role in the pathogenesis of diabetic nephropathy, Endocrine 35 (2009) 1–10.
[56] Y. Koyama, P. Wang, D.A. Brenner, T. Kisseleva, Stellate cells. portal myofibroblasts and epithelial-tomesenchymal transition, in: C.R. Gandhi, M. Pinzani (Eds.), Stellate cells in health and disease, Elsevier Inc., 2015, pp. 87–106.
[57] D. Hasegawa, M.C. Wallace, S.L. Friedman, Stellate cells and hepatic fibrosis, in: C.R. Gandhi, M. Pinzani (Eds.), Stellate cells in health and disease, Elsevier Inc., 2015, pp. 41–62.
[58] P. Pellicoro, P. Ramachandran, J.P. Iredale, J.A. Fallowfield, Liver fibrosis and repair: immune regulation of wound healing in a solid organ, Nat. Rev. Immunol. 14 (2014) 181–194.
[59] K. Kaji, H. Yoshiji, M. Kitade, Y. Ikenaka, R. Noguchi, Y. Shirai, Y. Aihara, T. Namisaki, J. Yoshii, K. Yanase, T. Tsujimoto, H. Kawaratani, H. Fukui, Combination treatment of angiotensin II type I receptor blocker and new oral iron chelator attenuates progression of nonalcoholic steatohepatitis in rats, Am. J. Physiol. Gastrointest. Liver Physiol. 300 (2011) G1094–G1104.
[60] Z. Bian, X. Ma, Liver fibrogenesis in nonalcoholic steato-hepatitis, Front. Physiol. 3 (2012) 248.
[61] E. Bugianesi, P. Manzini, S. D'Antico, E. Vanni, F. Longo, M. leone, P. Massarenti, A. Piga, G. Marchesini, M. Rizzetto, Relative contribution of iron burden, HFE mutations, and insulin resistance to fibrosis in nonalcoholic fatty liver, Hepatology 39 (2004) 179–187.
[62] G.H. Koek, P.R. Liedorp, A. Bast, The role of oxidative stress in nonalcoholic steatohepatitis, Clin. Chim. Acta. 412 (2011) 1297–1305.
[63] C. Garcia-Ruiz, A. Colell, A. Morales, N. Kaplowitz, J.C. Fernandez Checa, Role of oxidative stress generated form the mitochondrial electron transport chain and mitochondrial glutathione status in loss of mitochondrial function and activation of transcription factor nuclear factor-kappa B: studies with isolated mitochondria and rat hepatocytes, Mol. Pharmacol. 48 (1995) 825–834.
[64] D. Thong-Ngam, S. Samuhasaneeto, O. Kulaputana, N. Klaikeaw, N-acetylcysteine attenuates oxidative stress and liver pathology in rats with nonalcoholic steatohepatitis, World J. Gastroenterol. 13 (2007) 5127–5132.
[65] I.A. Leclercq, Antioxidant defence mechanisms: new players in the pathogenesis of nonalcoholic steatohepatitis, Clin. Sci. Lond. 106 (2004) 235–237.
[66] R. Crescenzo, F. Bianco, I. Falcone, P. Coppola, G. Liverini, S. Iossa, Increased hepatic de novo lipogenesis and mitochondrial efficiency in a model of obesity induced by diets rich in fructose, Eur. J. Nutr. 52 (2013) 537–545.
[67] P. Pasko, H. Barton, P. Zagrodzki, A. Izewska, M. Krosniak, M. Gawlik, M. Gawlik, S. Gorinstein, Effect of diet supplemented with quinoa seeds on oxidative status in plasma and selected tissues of high fructose-fed rats, Plant. Foods. Hum. Nutr. 65 (2010) 146–151.
[68] F. Francini, M.C. Castro, G. Schinella, M.E. Garcia, B. Maiztegui, M.A. Raschia, J.J. Gagliardino, M.L. Massa, Changes induced by a fructose-rich diet on hepatic metabolism and the antioxidant system, Life. Sci. 86 (2010) 965–971.
[69] A. Girard, S. Madani, F. Boukortt, M. Cherkaoui-Malki, J. Belleville, J. Prost, Fructose-enriched diet modifies antioxidant status and lipid metabolism in spontaneously hypertensive rats, Nutrition 22 (2006) 758–766.